

# CAMELOT

## UNDERSTANDING CHARGE, MASS AND HEAT TRANSFER IN FUEL CELLS FOR TRANSPORT APPLICATIONS

**Grant agreement no.: 875155**

**Start date:** 01.01.2020 – **Duration:** 36 months

**Project Coordinator:** Dr. Thor Aarhaug - SINTEF

### DELIVERABLE REPORT

<b>DELIVERABLE 4.1 – DOCUMENT DETAILING TESTING USED TO PARAMETERISE FFC</b>		
Due Date	30.06.2020	
Author (s)	Patrick Fortin, Alejandro O. Barnett	
Workpackage	WP4	
Workpackage Leader	Alejandro O. Barnett, SINTEF	
Quality Assurance	Thor Anders Aarhaug, SINTEF	
Date released by WP leader	29.06.2020	
Date released by Coordinator	29.06.2020	
<b>DISSEMINATION LEVEL</b>		
<b>PU</b>	Public	<b>X</b>
<b>PP</b>	Restricted to other programme participants (including the Commission Services)	
<b>RE</b>	Restricted to a group specified by the consortium (including the Commission Services)	
<b>CO</b>	Confidential, only for members of the consortium (including the Commission Services)	
<b>NATURE OF THE DELIVERABLE</b>		
<b>R</b>	Report	<b>X</b>
<b>P</b>	Prototype	
<b>D</b>	Demonstrator	
<b>O</b>	Other	

<b>SUMMARY</b>	
<b>Keywords</b>	Proton Exchange Fuel Cells (PEMFCs); Operating Conditions; Testing Protocols; Electrochemical Impedance Spectroscopy; Cyclic Voltammetry
<b>Abstract</b>	This document outlines the experimental protocols to be used throughout the CAMELOT project. Detailed descriptions of various <i>ex-situ</i> techniques used to characterise the electrochemical properties of the catalyst and physical properties of the electrode layers, <i>in-situ</i> techniques for the electrochemical characterisation of the membrane electrode assemblies (MEAs), as well as experimental conditions and procedures are provided. The protocols outlined in this report will serve to parameterise state-of-the-art PEMFCs, thus providing valuable input for improving future iterations of the open-sourced Fast-FC™ model and ultimately leading to a better understanding of the fundamental transport phenomena within low temperature proton exchange membrane fuel cells.
<b>Public abstract for confidential deliverables</b>	

<b>REVISIONS</b>			
Version	Date	Changed by	Comments

## D4.1 DOCUMENT DETAILING TESTING USED TO PARAMETERISE FFC

### CONTENT

1	Introduction .....	4
2	Scope.....	4
3	<i>Ex-Situ</i> Catalyst Characterisation .....	4
4	Structural Characterisation of Electrodes.....	6
5	Components, Conditions, and Protocols .....	10
6	<i>In-Situ</i> Electrochemical Characterisation Techniques .....	14
7	Conclusions and Future Work.....	20
8	References .....	20

## 1 INTRODUCTION

Proton Exchange Membrane Fuel Cells (PEMFCs) due to their high energy density, low operating temperature and high efficiency are considered to be very suitable for zero-emission vehicle propulsion. The overall aim of the CAMELOT project is to improve the power density of fuel cells by understanding the limitations on the performance of state-of-the-art (SoA) and beyond SoA PEMFC MEAs. To achieve this, the CAMELOT project will diagnose the fundamental transport properties that limit performance of these MEAs and materials. Furthermore, the CAMELOT project will not only produce MEAs with features that have the potential to enable disruptive performance increases but will further develop leading open source model to enable the accurate simulation validated through experimental work.

In depth *ex-situ* and *in-situ* characterisation is planned for a wide range of fuel cell material and components. This report includes a wide range of characterisation techniques and protocols that will be used throughout the CAMELOT project.

## 2 SCOPE

The Scope of this report is to provide the CAMELOT consortium with a plan and guidelines for the experimental work carried out in the project. The report contains general and detailed descriptions of a wide range of physical characterisation techniques to be used to characterize the CAMELOT fuel cell components, e.g. FIB-SEM and reconstruction of catalysts layers and MPLs. The report also contains general and detailed information of *in-situ* measurements techniques and protocols of for the characterisation of MEAs produced within the project.

**SINTEF**, **FCP**, **JMFC** and **IMTEK** will review this document every 6 months, to ensure that all necessary characterisation is performed as new materials and models become available. The JRC joint harmonised testing protocols are used as far as possible.

## 3 EX-SITU CATALYST CHARACTERISATION

### Rotating Disk Electrode (RDE) and Rotating Ring Disk Electrode (RRDE)

In general, a rotating disk electrode (RDE) can be described as a hydrodynamic working electrode whereby the rotation of the working electrode induces a flux of analyte to the electrode. When employed in a conventional three-electrode measurement, the rotating disk electrode allows for the determination of kinetic data such as Tafel slopes, reaction orders, and apparent activation enthalpies in the absence of mass transport effects. A variation of the RDE method, known as rotating ring disk electrode (RRDE), employs a second working electrode in the form of a ring that surrounds the central disk electrode. This second ring electrode is an independently controlled working electrode and measurements at the ring electrode allow for the determination of product distribution from the central electrode (e.g.,  $O_2:H_2O_2$  ratio during the ORR), which can provide valuable insight into reaction mechanisms at the central electrode. This technique is relevant for fuel cell catalyst studies as typical catalyst:ionomer inks can be coated onto planar conductive substrates (e.g., glassy carbon), resulting in the formation of a thin electrode layer resembling that of a fuel cell electrode. RDE measurements can, therefore, provide *ex-situ* characterisation of fuel cell catalyst kinetics in the absence of mass transport effects.

### Ink and Thin-Film Fabrication

In general, a typical catalyst ink consisting of solvent (e.g., a mixture of  $H_2O$  and IPA), catalyst (e.g., Pt/C), and ionomer (e.g., Nafion D520 dispersion) should be prepared and then further diluted to ensure catalyst layers with loading of  $10-30 \mu g_{Pt}/cm^2$  are formed on the disk electrode. Homogeneous catalyst layers can be achieved by drying the electrode under slow rotation of the disk electrode (e.g., at 700 rpm). For a detailed description of the experimental procedures, see the article from Martens *et al.* where universal preparation and testing conditions for RDE experiments are established to ensure reproducible results between labs.<sup>1</sup>

### Cell and Cleaning Procedure

Proper cleaning protocols are essential to avoid the presence of contaminants and ensure highly reproducible results. The glassy carbon disk electrode should first be polished using an alumina-particle suspension and then thoroughly rinsed in sequential DI water and IPA rinses. The electrochemical cell can be thoroughly cleaned by sequential soaks in a base bath, boiling water, and a 1:1 H<sub>2</sub>SO<sub>4</sub>:H<sub>2</sub>O<sub>2</sub> mixture; followed by thorough rinsing and boiling in water; and a final acid rinse (e.g., nitric or sulfuric acid).

### Protocol Details: CV, EIS, and LSV

See Martens *et al.* for detailed experimental procedures.<sup>1</sup> In general, RDE measurements should be performed in 0.1 M HClO<sub>4</sub> and at a rotation speed of 1600 rpm. Electrochemically active surface area (ECSA) determination and electrolyte resistance measurements by EIS should be performed with the cell headspace under inert atmosphere. ORR testing is performed under O<sub>2</sub> in the headspace.

To condition the catalyst layer, 100 potential cycles are performed between 0.05 V and 1.00 V (vs. RHE) at a sweep rate of 100 mV/s.

For ECSA determination, potential is cycled between 0.05 V and 1.00 V (vs. RHE) at a sweep rate of 20 mV/s for three cycles. The charge from the hydrogen desorption peak is calculated from 0.05 V to 0.4 V and used to calculate the ECSA (see section 6 for more detail regarding ECSA determination).

EIS can be used to determine the electrolyte resistance. A potential of 0.5 V is applied for 1 min, followed by an impedance measurement from 100,000 Hz to 10 Hz at an AC amplitude of 10 mV. The electrolyte resistance is determined by extrapolation of the linear part of the Nyquist plot to  $-Z_{im} = 0$ .

### Catalyst Activity

To determine catalyst activity towards the ORR, linear potential sweeps from 0.05 V to 1.00 V (vs. RHE) at a sweep rate of 5 mV/s are used. Background measurements should first be taken under inert atmosphere, followed by ORR tests under O<sub>2</sub>.

### Floating Electrode

Catalyst ink is applied onto a porous Au-coated polycarbonate membrane floating on the electrolyte. Oxygen can reach the catalyst directly through the membrane pores from the gas phase, enhancing mass transport by several orders of magnitude compared to the RDE. Floating electrode measurements are, therefore, similar to RDE measurements but have the advantage of characterizing catalyst layers at much higher overpotentials and current densities. Fabrication and electrochemical testing using the floating electrode technique should follow the procedures outlined by Martens *et al.*<sup>1</sup>

In general, floating electrode measurements should be performed in 1 M HClO<sub>4</sub> to minimize the potential drop across the solution between the working and reference electrodes. The catalyst layer is conditioned using 25 potential cycles between 0.05 V and 1.00 V (vs. RHE) under an inert atmosphere. Hydrogen is then flowed over the headspace and two voltammograms are collected between -0.1 V and 1.0 V. The headspace is replaced with oxygen and two voltammograms are collected between 1.0 V and 0.0 V. This entire procedure is repeated until the voltammograms collected under H<sub>2</sub> and O<sub>2</sub> are stable.

ORR performance is examined by collecting two voltammograms from 1.0 V to 0.0 V under O<sub>2</sub>, followed by a CV under inert atmosphere to collect capacitive background current.

ECSA determination is carried out under inert atmosphere, and the potential is cycled from 0.05 V to 1.00 V (vs. RHE).

Impedance measurements for iR correction are performed by applying a potential of 0.5 V for 1 min, followed by an impedance measurement from 100,000 Hz to 10 Hz at an AC amplitude of 10 mV. The electrolyte resistance is determined by extrapolation of the high frequency part of the Nyquist plot to  $-Z_{im} = 0$ .

In CAMELOT, most of the required *ex-situ* catalyst data has already been obtained by JFMC. Should the project require additional *ex-situ* catalyst characterisation, RDE and floating electrode measurements will be conducted as needed.

## 4 STRUCTURAL CHARACTERISATION OF ELECTRODES

### Scanning Electron Microscopy (SEM)

Scanning electron microscopy is a non-quantitative imaging technique that is used to visualize the macrostructure of the catalyst layer, as well as various macroscopic features of the MEA. Typical SEM analysis for fuel cell characterisation includes imaging of the catalyst layer structure (e.g., carbon support structure, catalyst distribution, porosity, layer thickness, surface roughness, cracks, and pinhole formation), the polymer membrane (e.g., thickness, catalyst particle migration, swelling behaviour), and the GDL (e.g., porosity).

In CAMELOT, SEM will be used to characterise new catalyst layer structures that will be subjected to *in-situ* characterisation. Specifically, SEM imaging will be used to determine membrane, anode, and cathode thickness, as well as thickness distribution. Select MEAs which have undergone *in-situ* fuel cell testing and AST protocols will undergo post-mortem analysis by SEM.

### Energy Dispersive X-Ray Spectroscopy (EDX)

EDX is an analytical technique that maps the elemental composition of a sample and can determine the relative abundance of each element within the sample. EDX detectors are often used in tandem with SEM. EDX can be used to study the degradation of catalyst layer, GDL, and coated bipolar plates over time by monitoring the change in elemental composition of each layer due to, for example, particle migration, growth and washing-out of catalyst particles. Alternatively, changes in the elemental composition may also be due the contamination of fuel cell components during fuel cell operation.

In CAMELOT, EDX analysis will be performed in concert with SEM imaging to analyse the elemental composition of the catalyst layer. More specifically, EDX will be used to examine changes in elemental distribution within the catalyst layer before and after AST testing.

### Focused Ion Beam Scanning Electron Microscopy (FIB-SEM)

FIB-SEM allows for the reconstruction of a high-resolution, three-dimensional image or model of the catalyst layer (or MPL) through the sequential FIB milling and SEM imaging of the sample. This technique represents a semi-quantitative method of studying catalyst layer morphology. The reconstruction of the catalyst layer structure then allows extraction of structural parameters and assessment of local gas diffusion and water transport inside the catalyst layer. In contrast to bulk methods such as BET or MIP, tomographic reconstruction allows differentiation between specific regions of the catalyst layer at different locations within the layer. This is key to investigating the ultrathin X-Y-Z catalyst layers envisioned in this project.

To properly resolve the structure of the catalyst layer with agglomerates in the range of 50 - 300 nm, the tomography requires a resolution of at least 20 nm. While SEM typically can resolve even below 1 nm, the FIB milling lies in the range of 5 – 30 nm depending on the material, current and milling ions. In Camelot, a very new FIB type shall be employed that utilizes a Xenon-Plasma for the ablation of material. This PFIB (Plasma FIB) has the advantage of significantly faster milling, no ion implementation in the sample, while meeting the required 20 nm milling distance to resolve the catalyst layer. IMTEK is one of the few institutions that has a PFIB already in place.

As tomographic reconstruction can still be very time consuming, tomographies shall only be employed when necessary. The approach followed in Camelot is to use the PFIB to create high-quality cross-sections of desired regions in the catalyst layer. Using the advantage of fast milling, large cross-sections can be obtained in order to analyse representative volumes (of few  $\mu\text{m}$ ) and have statistically meaningful results. This prevents the common mistake of high-resolution imaging with insufficient data. To assess three-dimensional transport properties from two-dimensional cross-sections the Bruggemann relation can be used as shown in literature (coefficient of 0.5).<sup>2</sup>

In another step, cross-section can also be lifted out and investigated in STEM mode (scanning transmission electron microscopy). This allows evaluating the catalyst loading, particle size, position on the carbon but also carbon. EDX performed on lift-out cross-sections have a significantly higher resolution of below 100 nm compared to several  $\mu\text{m}$  in normal EDX. Again, this is vital for the examination of catalyst layers with material gradients in all dimensions.

In summary, FIB-SEM is a powerful method that is inevitable to assess material gradients at desired locations of the XYZ-gradient catalyst layers envisioned in Camelot.

### Optical Profilometry and Micro-Computed Tomography

Micro-computed Tomography is a 3D imaging technique often used to measure the porosity of the gas diffusion layers. This technique offers non-destructive measurements with high spatial resolution and does not require the use of an intrusion fluid. A 3D reconstruction of the GDL microstructure is constructed by compiling individual scans obtained sequentially after a small rotation step. The porosity of the sample can then be calculated using dedicated software.

Optical profilometry complements micro-CT measurements by evaluating the surface roughness of the GDL. The use of light as a probe, as opposed to a physical stylus, ensures the surface of the sample is not altered or deformed.

In CAMELOT, contact area recreation between the GDL and BPP afforded through these techniques can be used to improve the contact resistance and tribology codes of the existing model.

### Mercury Porosimetry

Mercury intrusion porosimetry can be used to measure the total porosity (i.e., volume) and pore size distribution of the catalyst layer and GDL. In mercury intrusion porosimetry, mercury is introduced to the sample chamber and the application of a differential pressure forces mercury to fill the porous sample. As mercury does not preferentially wet either hydrophilic or hydrophobic pores, due to a large contact angle, it will not spontaneously infiltrate the porous sample. The measured intrusion volume is equal to the pore volume and the differential intrusion pressure is related to pore diameter by:

$$P_L - P_G = 4\sigma \frac{\cos \theta}{d_p}$$

where  $P_L$  is the pressure of the liquid,  $P_G$  is the pressure of the gas,  $\sigma$  is the surface tension of mercury,  $\theta$  is the contact angle of mercury and  $d_p$  is pore diameter.

A typical mercury intrusion porosimetry test involves placing a porous sample (e.g., CCM or GDL) into the sample chamber, evacuating the sample chamber to remove any gases or water vapour, and introducing mercury to the evacuated chamber. The sample chamber now contains the solid, porous sample; non-wetting liquid mercury; and mercury vapor. Next, the pressure in the sample chamber is slowly increased and the volume of mercury entering the porous sample is monitored. Mercury porosimetry is capable of determining a wide range of pore sizes, from 100  $\mu\text{m}$  down to 3 nm.

In CAMELOT, mercury porosimetry will provide valuable information regarding catalyst layer and GDL porosity as inputs for the modelling activities.

### Hele-Shaw

The pseudo-Hele-Shaw experiment allows for the characterisation of the through-plane water flow behaviour through the GDL. This technique places a GDL between two transparent PDMS plates and injects a fluid, typically water, through a hole in the bottom plate. As the water diffuses through the GDL, optical imaging cameras are used to monitor the total area occupied by the injected fluid and the interface of the injected-displaced fluids (the displaced fluid is typically air). A saturation curve can be obtained by plotting the total occupied area as a function of time, while plotting the fluid–fluid interface vs time yields a front length curve. By examining the time dependant saturation and front length curves, insight into the water transport mechanism through the GDL can be gained, e.g., stable displacement, viscous fingering, or capillary fingering. Careful consideration of the injection conditions is required, however, as it has been shown that fluid injection pressure influences the fluid flow behaviour.<sup>3</sup>

### Sessile Drop

The sessile drop technique allows for the calculation of the surface energy of a solid surface. In PEM fuel cells, it is often used to characterize the surface properties of gas diffusion layers. Different experiments of varying complexity are available to researchers, each with their own advantages. The simplest experiment is contact angle goniometry, where a liquid droplet is deposited onto the surface of the sample and a high-resolution camera takes an optical image from which the static contact angle can be determined. Larger contact angles are indicative of higher hydrophobicity, therefore, a comparison of hydrophobicity can be made between materials by comparing their contact angles.

### Dynamic Vapour Sorption

Absorption and desorption processes related to water uptake can be studied using dynamic vapour sorption. Here, the mass of the sample is monitored over time as a function of RH and temperature. Typically, the sample is held at constant temperature and the RH of the gas passing over and around the sample controlled. The RH is increased in a series of steps whilst the mass of the sample is monitored, such that both the gain in mass and the rate of mass gain can be measured. Depending on the instrument, RHs of up to about 90% can be used and series of measurements at increasing and then decreasing RH values can be used to construct water sorption isotherms. The technique is suitable for carbons, catalysts, catalyst layers and membranes. The method allows the water affinity of the different materials to be assessed and these can then be correlated with the behaviour of the components in the MEA under wet and dry operating conditions.

### Water Intrusion

The water intrusion method involves immersing a porous sample in water, where the water will spontaneously fill any hydrophilic pores, but will not enter any hydrophobic pores. As a differential pressure is applied to the sample chamber, the water will be forced into any hydrophobic pores. The volume of water forced into the pores is measured as a function of differential pressure. The volume of the hydrophobic pores is determined by the intrusion volume of water and the pore diameter can be calculated from Washburn's equation:

$$P_L - P_G = 4\sigma \frac{\cos \theta}{d_p}$$

where  $P_L$  is the pressure of the liquid,  $P_G$  is the pressure of the gas,  $\sigma$  is the surface tension of water,  $\theta$  is the contact angle of water and  $d_p$  is pore diameter.

### Gas Permeability

The through-plane gas permeability of a GDL can be measured by flowing nitrogen through the GDL and measuring the pressure drop across the GDL. This relationship is expressed by Darcy's law as:

$$\frac{\Delta p}{L} = \frac{\mu}{k} v$$

where  $\Delta p$  is the pressure drop across the sample,  $L$  is the thickness of the sample,  $\mu$  is the dynamic viscosity of nitrogen (in Pa s) at the temperature which the experiment is conducted,  $k$  is the gas permeability of the GDL, and  $v$  is the velocity of the flowing gas. Plotting the velocity of the flowing gas, i.e., the flow rate of nitrogen, (in  $\text{m s}^{-1}$ ) vs. the pressure gradient across the sample (in  $\text{Pa m}^{-1}$ ) yields a linear curve from which the gas permeability (in  $\text{m}^2$ ) can be extracted (i.e.,  $k = \mu/\text{slope}$ ).

### Heat Flux Measurements

Significant heat is produced alongside the production of water during the ORR at the cathode. Understanding the heat flux through the various components of a PEMFC, and through the fuel cell as a whole, can provide valuable insight into the governing kinetics and the water management within the cell.<sup>4</sup>

In CAMLEOT, this work will be subcontracted to the groups of Prof. Odne Burheim and Prof. Bruno Pollet at NTNU. They are able to measure the thermal conductivity of various fuel cell components using a custom built measurement rig designed to apply a constant heat flux through a cylindrical geometry that is symmetrical on the top and bottom.<sup>4</sup> The sample is placed between the hot upper side and the cold lower side of the rig and the thermal conductivity can be calculated using the relation between the heat flux and the temperature gradient, i.e., Fourier's law:

$$\kappa = -q_x \frac{\Delta T}{\Delta x}$$

where  $\kappa$  is the thermal conductivity,  $q_x$  is the heat flux in the x-direction, and  $\Delta T$  is the temperature change over the sample thickness,  $\Delta x$ . Taking the individual thermal conductivity values measured for each component, they are then able to produce a 2D model of heat distribution throughout the cell using the commercially available COSMOL Multiphysics software. A description of the model details is given in a review by Burheim.<sup>5</sup>

### Four-Probe Resistivity

The electronic resistance of various fuel cell components can be measured *via* the four-probe resistivity method. The resistance of a sample, with thickness 't', is measured by passing a DC current through the two outer probes, which induces a potential across the inner probes. Sheet resistance (in  $\Omega$ ) is measured by:

$$\rho = \frac{\pi E}{\ln 2 I}$$

where  $\rho$  is the sheet resistance,  $E$  is the measured potential across the inner probes, and  $I$  is the current applied to the outer probes.

The bulk resistance (in  $\Omega \cdot \text{cm}$ ) of the sample can also be calculated by multiplying the sheet resistance by the thickness of the sample.

In CAMELOT, the sheet resistance of the GDLs and catalyst layers will be measured *via* four-probe resistivity and used as input for the modelling activities.

### Contact Resistance

Interfacial contact resistance (ICR) measurements are useful for monitoring the degradation of metal bipolar plates as a result of being subjected to operating conditions of a fuel cell over time. The ICR measurements are conducted by placing the sample and a GDL between two gold-coated copper plates and applying a known current between the plates. At the center of the bottom plate, a small hole is present where a spring-loaded gold pin is used to contact the sample. The layered structure that is formed, from top to bottom, is as follows: top plate/GDL/sample/bottom plate. The gold pin is hooked up to a highly resistive voltmeter, ensuring that no current is passed through the gold pin, resulting in a negligible ICR between the sample and the gold pin. The voltage between the pin and the top plate is measured as a function of compaction force, from which the total ICR of the setup can be determined by Ohm's law. The total ICR can be expressed as the sum of the individual ICRs, that is:

$$R_T = R_{\text{gold-GDL}} + R_{\text{GDL/sample}}$$

As  $R_{\text{gold/GDL}}$  can be determined by repeating this experiment without the bipolar plate, the above equation can be rearranged to calculate  $R_{\text{GDL/sample}}$ .

The use of four terminals increases the accuracy of the voltage measurement, because the driving current is supplied from the power supply to the copper plates, but the voltage across the sample is measured by the sensing terminals connected by high-resistance cables to a multimeter. This way, the ohmic losses caused by the driving current have a much less of an impact on the voltage measurement. The accuracy of the measurement can be further improved by using a more powerful power supply (increasing the measured voltage and thus improving the signal-to-noise ratio) switched to a range resulting in the lowest possible error. Ideally, the sample should be kept at the expected operating temperature. It should be noted that as the GDL/sample sandwich settles, the reading will change over time, even under a constant compaction force.

In CAMELOT, contact resistance measurements will be carried out by SINTEF and the experimentally determined ICR values will be used as input for the modelling activities.

#### Four-Probe Impedance

The ionic conductivity of ion-exchange membranes can be calculated by:

$$\sigma = \frac{L}{AR}$$

where,  $\sigma$  is the membrane conductivity in S/cm,  $L$  is the distance between the two electrodes in cm,  $A$  is the cross-sectional area of the membrane in  $\text{cm}^2$ , and  $R$  is the measured membrane resistance in  $\Omega$ . Membrane resistance is determined by four-probe electrochemical impedance spectroscopy, where a hydrated membrane is clamped across four Pt strips. The inner Pt strips serve as voltage-sense probes and the outer Pt strips serve as AC current injectors. Membrane resistance is extracted from the low-frequency intercept of the real impedance axis of the Nyquist plot.

The four-probe method offers an advantage over the two-probe method in that the voltage-sense probes are separated from the current-sense probes, eliminating the interfacial resistance between the PEM and the Pt electrode. By eliminating the interference of interfacial impedance in the low-frequency region, the four-probe method can measure membrane resistance with greater accuracy.

In CAMELOT, the membrane conductivity will be used as input for the modelling activities.

## 5 COMPONENTS, CONDITIONS, AND PROTOCOLS

### Fuel Cell Components and Cell Hardware

CCMs: State-of-the-art CCMs, consisting of an ultrathin PFSA-based membrane (15  $\mu\text{m}$ ) and graded catalyst layers will be provided by Johnson Matthey. Pt loadings at the anode and cathode are 0.08  $\text{mg}_{\text{Pt}}/\text{cm}^2$  and 0.4  $\text{mg}_{\text{Pt}}/\text{cm}^2$ , respectively, where the anode has a nominal catalyst layer thickness of 8-10  $\mu\text{m}$  and the cathode has a nominal catalyst layer thickness of 10-12  $\mu\text{m}$ .

GDLs: Commercially available Sigracet 22BB GDLs will serve as the baseline GDLs used throughout the CAMELOT project.

Cell hardware: A lab-scale, single cell, quasi-1D test hardware will be used to accurately measure oxygen mass transport limitations.

### Standard Operating Conditions

The proposed operating conditions for the CAMELOT project will closely follow those outlined in the *EU Harmonised Test Protocols for PEMFC MEA Testing in Single Cell Configuration for Automotive Applications* report.<sup>6</sup> The proposed operating conditions are outlined in Table 5.1.

Table 5.1 Proposed fuel cell operating conditions for the CAMELOT project

	Parameters	Symbol	Unit	Values
	Nominal cell operating temperature	$T_{cell}$	°C	80
ANODE	Fuel gas inlet temperature	$T_{an}$	°C	85
	Fuel gas inlet humidity	$RH_{an}$	% RH	50
		$DP_{an}$	°C	64 (@ 80 °C)
	Fuel gas inlet pressure (absolute)	$p_{an}$	bar	2.5
	Fuel gas composition	-	-	H <sub>2</sub> (5.0 quality)
	Fuel stoichiometry	$\lambda_{an}$	-	1.3
CATHODE	Oxidant gas inlet temperature	$T_{cat}$	°C	85
	Oxidant gas inlet humidity	$RH_{cat}$	% RH	30
		$DP_{cat}$	°C	53 (@ 80 °C)
	Oxidant gas inlet pressure (absolute)	$p_{cat}$	bar	2.3
	Oxidant composition	-	-	Compressed air
	Cathode stoichiometry	$\lambda_{cat}$	-	2.0
Minimum current density for stoichiometry operation	$i_{\lambda min}$		A/cm <sup>2</sup>	0.2

### Stressor Operating Conditions

In addition to the standard operating conditions, high and low stressor conditions may be used to examine the physicochemical properties of the MEA under extreme conditions. Various high and low conditions for the operating variables of interest are outlined in table 5.2, while table 5.3 illustrates the 9 different stressor experiments outlined by the JRC *EU Harmonized Test Protocols*.<sup>6</sup> The conditions that deviate from the standard operating conditions are highlighted in red.

Table 5.2 List of high and low stressor conditions

Parameter	Low Condition	High Condition
Cell Temperature	45 °C	95 °C
Relative Humidity (Anode)	25 %RH	85 %RH
Relative Humidity (Cathode)	20 %RH	85 %RH
Fuel (H <sub>2</sub> ) stoichiometry	1.1	1.5
Oxidant (Air) stoichiometry	1.3	2.0
Backpressure (Anode)	1.6 bar <sub>abs</sub>	3.0 bar <sub>abs</sub>
Backpressure (Cathode)	1.4 bar <sub>abs</sub>	2.8 bar <sub>abs</sub>

Table 5.3 Stressor condition experiments as outlined by the JRC

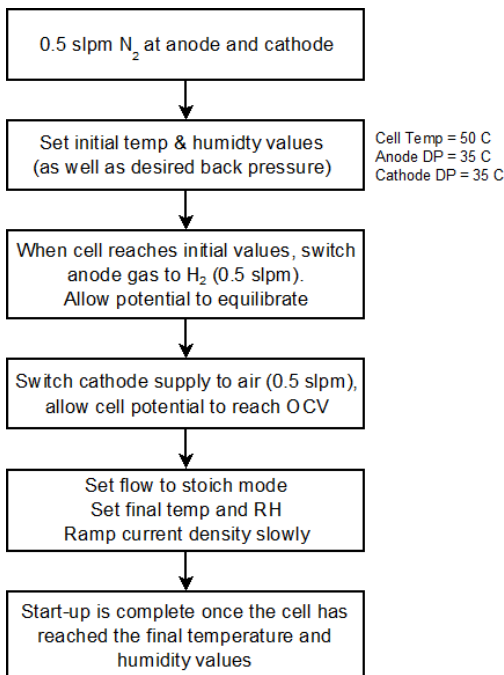
Test		$T_{cell}$ (°C)	$RH_{an}$ (%)	$p_{an}$ (bar <sub>abs</sub> )	$\lambda_{an}$	$RH_{cat}$ (%)	$p_{cat}$ (bar <sub>abs</sub> )	$\lambda_{cat}$
<i>Standard</i>		80	50	2.5	1.3	30	2.3	1.5
$T_{cell}$	Cold & Wet	45	85	2.5	1.3	85	2.3	1.5
	Hot & Dry	95	25	2.5	1.3	20	2.3	1.5
$RH$	Dry Membrane	95	50	2.5	1.3	20	2.3	1.5
	High RH Difference	95	25	2.5	1.3	45	2.3	1.5
	Cathode Flooding	80	50	2.5	1.3	45	2.3	1.5
<i>Backpressure</i>	Low Backpressure	80	50	1.6	1.3	30	1.4	1.5
	High Backpressure	80	50	3.0	1.3	30	2.8	1.5
<i>Stoichiometry</i>	Low Stoichiometry	80	50	2.5	1.3	30	2.3	1.3
	High Stoichiometry	80	50	2.5	1.3	30	2.3	2.0

**Break-In Procedure**

The break-in procedure to be used in CAMELOT consists of holding the cell at a constant current of 500 mA/cm<sup>2</sup> for 16 hours at 100% RH, 80 °C, and 1 bar back pressure at both the anode and cathode. The break-in procedure is to be performed under H<sub>2</sub> at the anode (stoich 1.5) and air at the cathode (stoich 2).

**Start-Up Procedure**

The start-up procedure intends to protect the cathode catalyst layer from high potentials leading to carbon corrosion.



- The dewpoint of both the anode and cathode should be set at a temperature that always ensure the dew point temperature does not exceed the cell temperature at any point during the start-up procedure. This ensures the prevention of liquid water condensation within the catalyst layer during startup.

- Gas flow at both the anode and cathode should begin under N<sub>2</sub> and at a flow rate of 0.5 Nlpm.

- Once the fuel cell has reached the desired operating temperature and relative humidity, the anode gas may be switched to hydrogen. The fuel cell is now ready for electrochemical characterisation. The cathode compartment may remain under N<sub>2</sub> or can be switched to air, depending on the desired experimental procedure (see sections 5.2.5 and 5.3 for further details).

### Shutdown Procedure

As for the start-up procedure, the shutdown procedure intends to protect the cathode catalyst layer from high potentials leading to carbon corrosion.

-Reduce and remove load. Note: Gas flow should be switched to the minimum flow as defined by the standard operating procedures (see Table 5.1).

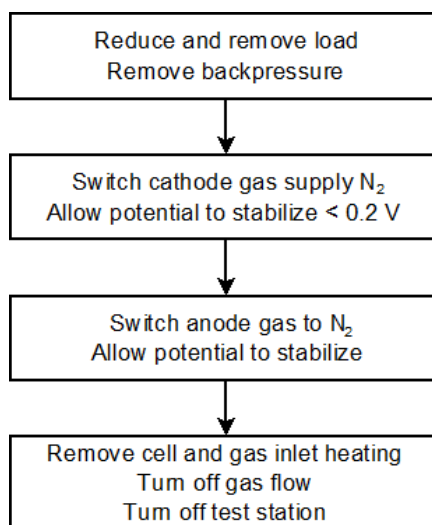
-Remove backpressure

-Switch the cathode gas feed to N<sub>2</sub> and allow cell voltage to stabilize <0.2 V. This ensures that the majority of the oxygen has been removed from the cathode compartment, preventing fuel starvation and subsequent irreversible degradation. A small current can be applied here to promote the electrochemical reduction of residual oxygen at the cathode, thereby speeding up the removal of oxygen through consumption.

-The anode gas feed can be switched to N<sub>2</sub>. Once the cell voltage is stable, gas flows can be turned off.

-Remove cell and gas inlet heating.

-Turn off the test station.



A small current can be applied to promote the electrochemical reduction of residual oxygen at the cathode. Ensure cell potential does not reach dangerously low levels.

### Characterisation Protocol

Fuel cell characterisation will follow the protocols outlined in section 6 *In-Situ electrochemical characterisation techniques*.

### Accelerated Stress Test Protocol

The accelerated stress test protocols employed in the CAMELOT project will follow the procedures outlined by the US DoE.

### Electrocatalyst AST

The durability of catalysts can be compromised by platinum sintering, particle growth, and dissolution, especially at high electrode potentials. This sintering/dissolution is accelerated under load-cycling. The AST for the electrocatalyst specifies load cycling from 0.6 V to 0.95 V at a sweep rate of 50 mV/s for 30,000 cycles or until catalytic activity loss reaches 40%, the electrochemical surface area (ECSA) decreases by 40%, or performance is reduced by 30 mV at 0.8 A/cm<sup>2</sup>. The AST should be performed at a cell temperature of 80 °C, 100% RH at both the anode and cathode, H<sub>2</sub> at the anode with a flow rate of 0.2 Nlpm, N<sub>2</sub> at the cathode with a flow rate of 0.075 Nlpm, and no back pressure. Polarization curves should be collected after 0, 1k, 5k, 10k, and 30k cycles.

ECSA data should be collected after 1k, 5k, 10k, and 30k cycles. CO-stripping should be used for ECSA determination (see section 6 for experimental details).

### Catalyst Support AST

The AST for catalyst supports specifies load cycling between 1.0 V and 1.5 V at a sweep rate of 500 mV/s for 5000 cycles or until catalytic activity loss reaches 30 %, the electrochemical surface area (ECSA) decreases by 40 %, or performance is reduced by 30 mV at 1.5 A/cm<sup>2</sup>. The AST should be performed at a cell temperature of 80 °C, 100 % RH at both the anode and cathode, H<sub>2</sub> at the anode, and N<sub>2</sub> at the cathode.

Polarization curves should be collected after 0, 100, 200, 500, 1k, 2k, and 5k cycles.

ECSA data should be collected after 0, 100, 200, 500, 1k, 2k, and 5k cycles. CO-stripping should be used for ECSA determination (see section 6 for experimental details).

#### MEA Chemical Stability AST

The AST for MEA chemical stability specifies a steady state OCV hold for 500 hours, or until OCV decays by 20 %, or H<sub>2</sub> crossover increases beyond 2mA/cm<sup>2</sup>. The AST should be performed at a cell temperature of 90 °C, 30 % RH at both the anode and cathode, H<sub>2</sub> at the anode, and air at the cathode. Gas flow stoichs should be equal to 10 at an equivalent flow at 0.2 A/cm<sup>2</sup>. Backpressure should be 0.5 bar<sub>g</sub> at both anode and cathode.

Fluoride ion release (or equivalent for hydrocarbon membranes) should be monitored every 24 hours. HFR resistance should be measured every 24 hours, at 0.2 A/cm<sup>2</sup>, and H<sub>2</sub> crossover should be monitored every 24 hours until crossover current exceeds 2 mA/cm<sup>2</sup>.

#### Membrane Mechanical AST

RH cycling results in swelling of the membrane as it absorbs water at high RH and shrinks as it loses water at low RH. This swell/shrink cycling results in high mechanical stresses in the membrane and subsequent mechanical failure resulting in gas crossover across the membrane. The AST for the mechanical degradation of the membrane specifies RH cycling from 0 %, for 2 mins, to a dew point of 90 °C (saturated RH), for 2 mins, for a total of 20000 cycles or until crossover current exceeds 2 mA/cm<sup>2</sup>. The AST should be performed at 80 °C, under H<sub>2</sub> and air, with flow rates of 2 Nlpm for both gases, and no backpressure.

## 6 IN-SITU ELECTROCHEMICAL CHARACTERISATION TECHNIQUES

### Cyclic Voltammetry and CO-stripping

Cyclic voltammetry is an electrochemical characterisation technique commonly employed in fuel cell testing to assess the electrochemically active surface area (ECSA) of the Pt catalyst in fuel cell electrodes, an important performance metric that provides an estimate of catalyst utilisation and degradation. Cyclic voltammetry is an in-situ technique most commonly applied to single cells and it is well covered in the literature.<sup>7</sup> In CAMELOT, CO-stripping voltammetry will be employed for ECSA determination as it has been shown to be more accurate than the more commonly used hydrogen adsorption/desorption voltammetry, especially for small Pt nanoparticle catalysts and Pt-alloy nanoparticle catalysts.

Diluted hydrogen (e.g., 5 % H<sub>2</sub> in N<sub>2</sub>) is usually used on the anode side of the cell, while diluted CO (e.g., 1 % CO in N<sub>2</sub>) is purged over the cathode side to create an adsorbed CO monolayer on the cathode catalyst, followed by an N<sub>2</sub> purge to remove any remaining CO. In this case, the CO containing side is connected as the working electrode and the H<sub>2</sub> containing electrode functions as a pseudoreference electrode and connected as counter/reference electrode. Diluted H<sub>2</sub> is preferred in order to avoid high hydrogen crossover rates influencing the shape of the voltammogram. In addition, repetitive cycling to high voltage may also degrade the working electrode. Therefore, it is important to limit the number of cycles as well as the higher potential limit while still being able to extract important information from these measurements.

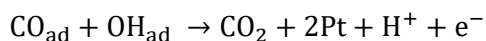
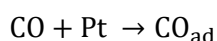
Table 6.1 shows a set of operating conditions, for the evaluation of lab-scale single cells.

Table 6.1 Operating conditions for ECSA determination via CO-stripping voltammetry

	Parameter	Symbol	Unit	Conditions
	Nominal cell operating temperature	T	°C	80
Counter/ reference	Fuel gas inlet temperature	T	°C	85
	Fuel gas inlet humidity	RH	%	100
	Fuel gas inlet pressure (absolute)	p	bar	2.0
	H <sub>2</sub> flow rate	Nlpm	NL min <sup>-1</sup>	1.0
Working	Oxidant gas inlet temperature	T	°C	85
	Oxidant gas inlet humidity	RH	%	100
	Oxidant gas inlet pressure (absolute)	p	bar	2.0
	CO/N <sub>2</sub> flow rate	Nlpm	NL min <sup>-1</sup>	1.0

The proposed experimental protocol for performing the CO-stripping voltammetry (i.e., ECSA determination) is as follows:

1. Clean the catalyst surface by conducting 2 cycles of cyclic voltammetry between 0.05 and 0.85 V (vs. SHE) under N<sub>2</sub> on the cathode.
2. Adsorb CO by purging 1% CO (balanced with N<sub>2</sub>) to the cathode channel for 10 min while holding the potential at 0.125 V (vs. SHE).
3. Purge cathode channel with N<sub>2</sub> for 10 min to remove residual CO.
4. Perform CO stripping with 2 cycles of cyclic voltammetry between 0.05 and 0.85 V (vs. SHE) at a sweep rate of 50 mV/s. The first cycle of the CO stripping produces a distinct CO oxidation peak corresponding to the complete desorption by oxidation to CO<sub>2</sub> and the second cycle is used as a baseline from which we can calculate the area of the CO oxidation peak. Additional cycles can be performed to ensure the baseline is accurate. The measurement of ECSA by this method is based on the assumption that each molecule of CO is able to occupy one site on the available platinum surface, and that all sites that are active and accessible are occupied during the measurement. The CO adsorption and subsequent oxidation that occur at higher overpotentials on Pt sites can be described by the following chemical equations:<sup>8</sup>



The ECSA of the electrode in units of m<sup>2</sup>g<sup>-1</sup> is then calculated using the following formula:

$$ECSA = \frac{Q}{\Gamma_L} \tag{6.1}$$

where  $Q$  is the integrated charge density ( $C/cm^2$ ) calculated from the CO oxidation peak,  $\Gamma$  is the specific charge required to oxidize a monolayer of the adsorbed species (i.e.  $420 \mu C/cm^2$  for a two-electron transfer assuming the oxidation of one molecule of CO to  $CO_2$  per Pt atom), and  $L$  is the platinum loading of the electrode ( $g/m^2$ ).

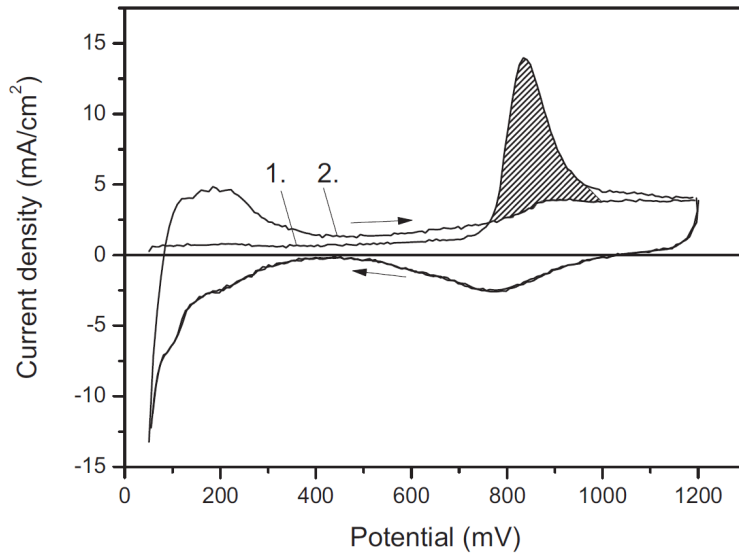


Figure 6.1 A typical CO-stripping voltammogram of a PEMFC where sweep 1 represents the CO stripping process and sweep 2 represents the baseline.<sup>9</sup> The region of interest used in calculating the charge associated with the CO oxidation process is indicated by the shaded area.

### EIS Under $N_2$

Electrochemical impedance spectroscopy (EIS) is regarded as a suitable electrochemical characterisation technique for studying fuel cell performance. During these measurements, a small sinusoidal current or voltage perturbation is applied at different frequencies which makes it possible to distinguish processes occurring at different time scales. However, in many situations a mathematical model is needed to increase the knowledge of the investigated system, especially when different processes with approximately the same time constants occur simultaneously.

When EIS is performed with the cathode compartment under nitrogen, it is possible to discern the electrolytic resistance of the cathode catalyst layer, i.e., the protonic resistance of the ionomer present in the catalyst layer, from the difference between the low frequency and high frequency intercepts of the real impedance axis. The low frequency intercept can be approximated from the x-intercept extrapolated from a linear fit of the low-frequency data. The real impedance is equal to one-third of the electrolytic resistance of the catalyst layer:

$$Z' (\Omega) = \frac{R_{CL}}{3} \tag{6.2}$$

where  $Z'$  is the difference between the low-frequency and high-frequency intercepts of the real impedance axis and  $R_{CL}$  is the electrolytic resistance of the catalyst layer.

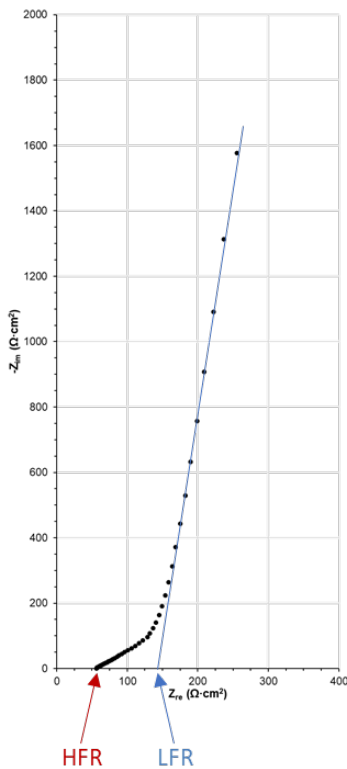


Figure 6.2. Typical Nyquist plot obtained when EIS is performed under N<sub>2</sub> at the cathode. HFR is the high frequency intercept and LFR is the low frequency intercept.

Additionally, the high-frequency intercept of the real impedance axis represents the Ohmic resistance of the cell.

When performing EIS under H<sub>2</sub>/N<sub>2</sub>, a potential should be chosen to ensure that the DC response is purely capacitive, i.e., there are no Faradaic contributions. A suitable potential can be chosen by examining a cyclic voltammogram performed under H<sub>2</sub>/N<sub>2</sub> and choosing a potential that falls within the purely capacitive region, but typically a potential of 0.5 V can be used to avoid contributions from Faradaic currents.<sup>10</sup>

### H<sub>2</sub> Crossover Measurements (Linear Sweep Voltammetry)

In fuel cell applications, linear sweep voltammetry (LSV) can be used to directly measure the amount of hydrogen gas crossing over from the anode compartment to the cathode compartment. Here, the cathode compartment is flushed with nitrogen (at a flowrate of 0.5 slpm), while the anode is kept under hydrogen (also at 0.5 slpm). Using an external potentiostat, the working electrode is hooked up to the nitrogen side of the cell, while the hydrogen side acts as the counter and reference electrode. When a potential is applied, any hydrogen that has crossed over to nitrogen-filled compartment is oxidized at the working electrode catalyst layer and a current can be measured. When a large enough potential is applied (typically 500 mV), all the hydrogen molecules that have made their way across the membrane will be oxidized by the working electrode catalyst layer, resulting in a limiting current density. This limiting current density is often reported as the measure of gas crossover or a crossover flux, expressed in mol cm<sup>-2</sup> s<sup>-1</sup>, and can be calculated using:

$$\text{flux} = \frac{i_{lim}}{nF} \tag{6.3}$$

where  $i_{lim}$  is the limiting current density, measured at 500 mV,  $n$  is the number of electrons involved in the electrochemical reaction (for the oxidation of hydrogen gas,  $n=2$ ), and  $F$  is Faraday's constant. Figure 6.3 illustrates the operation of a PEMFC under normal working conditions and when performing gas crossover measurements.<sup>11</sup>

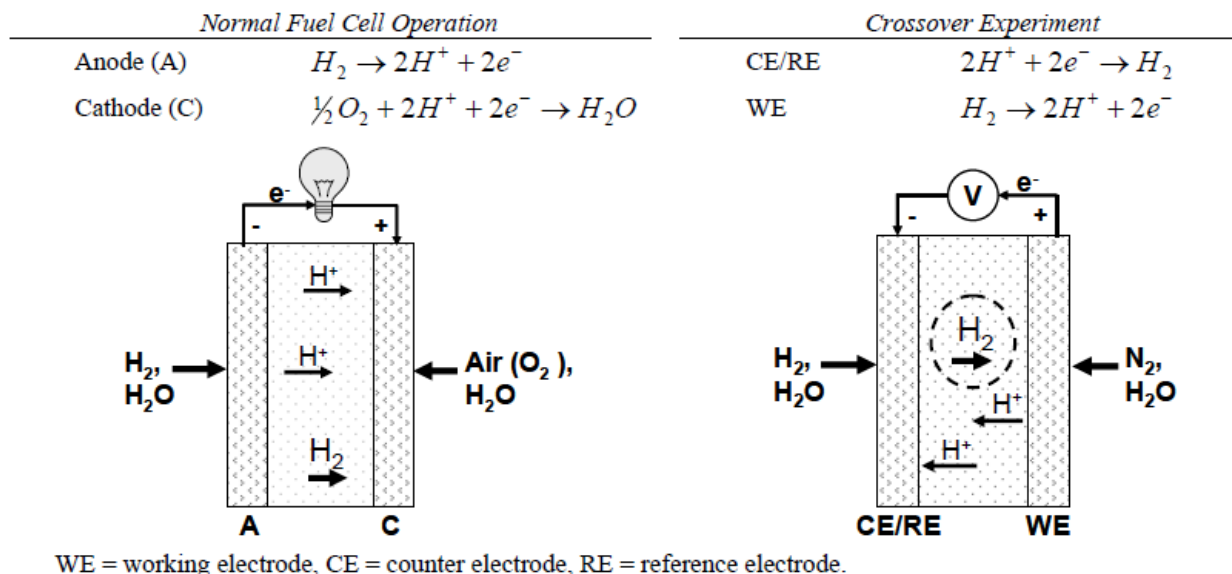


Figure 6.3. Schematic of a proton exchange membrane fuel cell operation under normal operation (left) and for gas crossover determination (right).<sup>11</sup>

A typical gas crossover measurement using LSV uses a sweep rate of  $1 \text{ mV s}^{-1}$  starting from a potential of 0.1 V until a potential of 0.6 V is reached and the current density value a potential of 500 mV is taken as the limiting current density.

Linear sweep voltammetry also has the ability to diagnose internal electrical shorts within the MEA. Typical LSV measurements should produce a voltammogram consisting of a flat limiting current density region at higher electrode potentials. The appearance of linearly increasing current densities with increasing potential is indicative of an internal electrical short, where the electrical resistance of the cell can be estimated from the slope of the voltammogram.<sup>11</sup>

### Polarisation Curves

The objective of performing polarization curve measurements is to determine the MEA performance in terms of cell voltage and power density against current density at specified operating conditions. The dwell time of each set point should be sufficiently long to ensure that stabilization criteria of cell voltage (e.g.,  $\pm 5 \text{ mV}$ ) are met. This typically means a dwell time of 2 min, and should not exceed 15 min. The exception is measurements performed at OCV, for which dwell times should not exceed 1 min. The following polarisation curve protocol is proposed for the CAMELOT project: based on the procedures outlined in the GAIA project:

- 1.) Pre-conditioning the cell at  $0.5 \text{ A/cm}^2$  for 3600 seconds.
- 2.) Lowering the current density to  $0.02 \text{ A/cm}^2$  for 300 seconds.
- 3.) Increasing the current density in  $0.02 \text{ A/cm}^2$  steps up to  $0.1 \text{ A/cm}^2$ , then increasing current density in  $0.1 \text{ A/cm}^2$  steps up to  $0.6 \text{ A/cm}^2$ , and finally increasing the current density in  $0.2 \text{ A/cm}^2$  steps up to  $3 \text{ A/cm}^2$  or cell voltage lower than 0.3 V. All current steps should have a dwell time of 300 seconds.
- 4.) Lowering the current density with different hold times.
- 5.) Holding OCV for 35 seconds.

### Polarisation Curves in O<sub>2</sub>

Polarisation data collected in pure oxygen allows the MEA to operate free from mass transport limitations due to oxygen supply constraints to the cathode catalyst layer. A comparison of polarisation curves collected with the cathode compartment under oxygen and under air can provide insight into oxygen mass transport limitations from the so-called "oxygen gain". Oxygen gain is the potential difference observed between the polarization curves collected under oxygen and air, as a function of current density. The evolution of oxygen gain over time can also provide information about the mass transport related degradation, e.g., increasing oxygen gain over time suggests an increase in mass transport losses within the cathode. Although oxygen gain experiments provide a simple method to estimate oxygen mass transport losses within a fuel cell, they are not capable of discerning the origin of these losses, e.g., in the GDL vs. the catalyst layer.

### Polarisation Curves in Air

Although the operation of a fuel cell with pure oxygen at the cathode compartment will provide the best performance, it is impractical for most applications. As a result, air is used to better represent real-life operational conditions in a fuel cell. As air can generally be thought of as O<sub>2</sub> diluted to 21 % v/v in N<sub>2</sub>, fuel cells operated with air at the cathode suffer from reduced thermodynamic potential ( $E_{\text{theor}} \propto \log(p_{\text{O}_2}^{1/2})$ ), reduced ORR kinetics (due to the concentration dependence of the exchange current density), and exacerbated mass transport limitations (especially at high current densities).

### Polarisation Curves in Helox

Polarisation measurements taken when the cathode gas composition is made up of O<sub>2</sub> with a balance of He (i.e., helox) can be used to determine the origin and contribution of various mass transport losses.<sup>12</sup> In general, O<sub>2</sub> mass transport losses belong to three categories: i) molecular diffusion, ii) Knudsen diffusion, and iii) permeation through the ionomer present in the catalyst layer. The dominant mode of mass transport in each layer of the MEA is dependent on pore size and composition. When pores are large, in the GDL for example, molecular diffusion dominates, while Knudsen diffusion is negligible (although Knudsen diffusion likely contributes, to some extent, in the MPL as the pore size decreases). As the oxidant gas flows from the GDL into the catalyst layer, Knudsen diffusion now dominates as the pore size of the catalyst layer is typically less than 100 nm. Finally, as O<sub>2</sub> must make its way to the Pt surface through the ionomer layer, the dominant transport resistance will be the permeability of O<sub>2</sub> through the ionomer.

By taking advantage of the pressure dependence of molecular diffusion and the change in O<sub>2</sub> diffusion coefficient in various balance gases, e.g., N<sub>2</sub> and He, it is possible to distinguish between mass transport limitations through the systematic variation of experimental conditions.

### EIS

Electrochemical impedance spectroscopy (EIS) is regarded as a suitable electrochemical characterisation technique for studying fuel cell performance. During these measurements a small sinusoidal current or voltage perturbation is applied at different frequencies which makes it possible to distinguish processes occurring at different time scales. However, in many situations a mathematical model is needed to increase the knowledge of the investigated system, especially when different processes with approximately the same time constants occur simultaneously.

When EIS is performed with the cathode under oxygen or air, it is possible to obtain both the Ohmic resistance of the cell, from the high frequency intercept, and the charge transfer resistance at the cathode catalyst layer. For an ideal system, the difference between the low-frequency and high-frequency intercepts of the real impedance axis (i.e., the width of the semi-circle) is used to calculate the charge transfer resistance. Often in real systems, more complicated mathematical models are needed to calculate the charge transfer resistance.

By performing EIS measurements after each current density step along the polarisation curve, ohmic resistance data is obtained that can be used to produce iR-corrected polarisation curves. Additionally, high quality EIS spectra

collected at three different current densities (e.g., 0.1, 0.8, and 1.8 A/cm<sup>2</sup>) representative of the three different regions along the polarization curve (i.e., activation, ohmic, and mass transport regions) is a useful way of examining the evolution of various resistances as local conditions change with current density.

## 7 CONCLUSIONS AND FUTURE WORK

This report outlines the various characterisation techniques to be employed over the duration of the CAMELOT project. The primary objective of these measurements is to determine the physicochemical properties of state-of-the-art fuel cell components, with an emphasis on membrane and catalyst layers, that will serve to elucidate their influence on mass transport and heat transfer through the fuel cell. The experimental results obtained through the methods outlined here will serve as valuable input for the modelling activities performed in WP2.

## 8 REFERENCES

- (1) Martens, S.; Asen, L.; Ercolano, G.; Dionigi, F.; Zalitis, C.; Hawkins, A.; Martinez Bonastre, A.; Seidl, L.; Knoll, A. C.; Sharman, J.; et al. A Comparison of Rotating Disc Electrode, Floating Electrode Technique and Membrane Electrode Assembly Measurements for Catalyst Testing. *J. Power Sources* **2018**, *392*, 274–284. <https://doi.org/10.1016/j.jpowsour.2018.04.084>.
- (2) Tjaden, B.; Cooper, S. J.; Brett, D. J.; Kramer, D.; Shearing, P. R. On the Origin and Application of the Bruggeman Correlation for Analysing Transport Phenomena in Electrochemical Systems. *Curr. Opin. Chem. Eng.* **2016**, *12*, 44–51. <https://doi.org/10.1016/j.coche.2016.02.006>.
- (3) Medici, E. F.; Allen, J. S. Existence of the Phase Drainage Diagram in Proton Exchange Membrane Fuel Cell Fibrous Diffusion Media. *J. Power Sources* **2009**, *191* (2), 417–427. <https://doi.org/10.1016/j.jpowsour.2009.02.050>.
- (4) Bock, R.; Karoliussen, H.; Pollet, B. G.; Secanell, M.; Seland, F.; Stanier, D.; Burheim, O. S. The Influence of Graphitization on the Thermal Conductivity of Catalyst Layers and Temperature Gradients in Proton Exchange Membrane Fuel Cells. *Int. J. Hydrogen Energy* **2020**, *45* (2), 1335–1342. <https://doi.org/10.1016/j.ijhydene.2018.10.221>.
- (5) Burheim, O. S. (Invited) Review: PEMFC Materials' Thermal Conductivity and Influence on Internal Temperature Profiles. *ECS Trans.* **2017**, *80* (8), 509–525. <https://doi.org/10.1149/08008.0509ecst>.
- (6) Tsotridis, G.; Pilenga, A.; Marco, G. De; Malkow, T. *EU Harmonised Test Protocols for PEMFC MEA Testing in Single Cell Configuration for Automotive Applications; JRC Science for Policy Report*; 2015. <https://doi.org/10.2790/54653>.
- (7) Lindström, R. W.; Kortsdotir, K.; Wesselmark, M.; Oyarce, A.; Lagergren, C.; Lindbergh, G. Active Area Determination of Porous Pt Electrodes Used in Polymer Electrolyte Fuel Cells: Temperature and Humidity Effects. *J. Electrochem. Soc.* **2010**, *157*, B1795. <https://doi.org/10.1149/1.3494220>.
- (8) Rudi, S.; Cui, C.; Gan, L.; Strasser, P. Comparative Study of the Electrocatalytically Active Surface Areas (ECSAs) of Pt Alloy Nanoparticles Evaluated by Hupd and CO-Stripping Voltammetry. *Electrocatalysis* **2014**, *5* (4), 408–418. <https://doi.org/10.1007/s12678-014-0205-2>.
- (9) Brightman, E.; Hinds, G.; O'Malley, R. In Situ Measurement of Active Catalyst Surface Area in Fuel Cell Stacks. *J. Power Sources* **2013**, *242*, 244–254. <https://doi.org/10.1016/j.jpowsour.2013.05.046>.
- (10) Makharia, R.; Mathias, M. F.; Baker, D. R. Measurement of Catalyst Layer Electrolyte Resistance in PEFCs Using Electrochemical Impedance Spectroscopy. *J. Electrochem. Soc.* **2005**, *152* (5), A970. <https://doi.org/10.1149/1.1888367>.
- (11) Cooper, K. R. In Situ PEMFC Fuel Crossover & Electrical Short Circuit Measurement. *Fuel Cell Magazine*. 2008, pp 1–2.
- (12) Nonoyama, N.; Okazaki, S.; Weber, A. Z.; Ikogi, Y.; Yoshida, T. Analysis of Oxygen-Transport Diffusion Resistance in Proton-Exchange-Membrane Fuel Cells. *J. Electrochem. Soc.* **2011**, *158* (4), B416. <https://doi.org/10.1149/1.3546038>.